

Adaptation of microbial resource allocation affects modeled long term soil organic matter and nutrient cycling

Thomas Wutzler^a, Sönke Zaehle^{a,b}, Marion Schrumpf^a, Bernhard Ahrens^a,
Markus Reichstein^{a,b}

^a*Max Planck Institute for Biogeochemistry, Hans-Knöll-Straße 10, 07745 Jena, Germany*

^b*Michael Stifel Center Jena for Data-driven and Simulation Science, Jena, Germany*

Abstract

In order to understand the coupling of carbon (C) and nitrogen (N) cycles, it is necessary to understand C and N-use efficiencies of microbial soil organic matter (SOM) decomposition. While important controls of those efficiencies by microbial community adaptations have been shown at the scale of a soil pore, an abstract simplified representation of community adaptations is needed at ecosystem scale.

Therefore we developed the soil enzyme allocation model (SEAM), which takes a holistic, partly optimality based approach to describe C and N dynamics at the spatial scale of an ecosystem and time-scales of years and longer. We explicitly modelled community adaptation strategies of resource allocation to extracellular enzymes and enzyme limitations on SOM decomposition. Using SEAM, we explored whether alternative strategy-hypotheses can have strong effects on SOM and inorganic N cycling.

Results from prototypical simulations and a calibration to observations of an intensive pasture site showed that the so-called revenue enzyme allocation strategy was most viable. This strategy accounts for microbial adaptations to

both, stoichiometry and amount of different SOM resources, and supported the largest microbial biomass under a wide range of conditions. Predictions of the holistic SEAM model were qualitatively similar to predictions of the SYMPHONY model, which explicitly represents competing microbial guilds. With adaptive enzyme allocation under conditions of high C/N ratio of litter inputs, N that was formerly locked in slowly degrading SOM pools was made accessible, whereas with high N inputs, N was sequestered in SOM and protected from leaching.

The findings imply that it is important for ecosystem scale models to account for adaptation of C and N use efficiencies in order to represent C-N couplings. The combination of stoichiometry and optimality principles is a promising route to yield simple formulations of such adaptations at community level suitable for incorporation into land surface models.

Keywords: soil, enzyme, model, stoichiometry, adaptation, microbe

1. Introduction

The global element cycles of carbon (C) and nitrogen (N) are strongly linked and cannot be understood without their intricate interactions (Thorn-ton et al., 2007; Janssens et al., 2010; Zaehle and Dalmonech, 2011). The ties between nutrient cycles are especially strong in the dynamics of soil organic matter (SOM), because the depolymerisation and mineralisation of SOM relies on a microbial decomposer community with a rather strict homeostatic regulation of their stoichiometry, i.e. their elemental ratio of C/N (Serner and Elser, 2002; Zechmeister-Boltenstern et al., 2015). Therefore, it is important to represent effects of microbial control on soil biogeochemistry also in

ecosystem to global scale models (Todd-Brown et al., 2012; Xu et al., 2014).

C and N fluxes controlled by microbial stoichiometry comprise respiration of organic C, mineralization of organic N, and immobilization of inorganic N. They occur if decomposers experience stoichiometric imbalance, i.e. differences in elemental composition between food and the requirement of feeders (Sterner and Elser, 2002). Decomposers require a certain amount of C for each unit of N. With balanced growth, i.e. when stoichiometry of the food matches the requirements, decomposers can utilize all food for productive purposes such as synthesis of new biomass or enzymes, growth respiration, and maintenance respiration. If there is different amount of C per unit N in the food, decomposers have to deal with this imbalance in some way.

Decomposers can - in principle - adjust in three different ways when faced with imbalances between the stoichiometry of the organic material (OM), i.e. the litter and SOM they feed on, and their own stoichiometric requirements (Mooshammer et al., 2014b). First, individual microbes can adapt their carbon-use efficiency (CUE), or their nutrient-use efficiency (Sinsabaugh et al., 2013). The alteration of CUE has shown to have large consequences on prediction of carbon sequestration in SOM (Allison, 2014; Wieder et al., 2013). Regulation of nutrient use efficiency has consequences for nutrient recycling and loss of nutrients from the ecosystem (Mooshammer et al., 2014a) and soil plant feedback (Rastetter, 2011). Second, decomposer communities can adapt their stoichiometric requirements. Community composition can shift between species with high C/N ratio, such as many fungi, or species with lower C/N ratio, such as many bacteria (Cleveland and Liptzin, 2007; Xu et al., 2013), although the flexibility is relatively narrow. Third,

36 decomposers can adapt their allocation of resources into synthesis of different
37 extracellular enzymes to preferentially degrade fractions of SOM that differ
38 by their stoichiometry (Moorhead et al., 2012).

39 Representation and consequences of stoichiometry on element cycling dif-
40 fer between models at different scales. Most models at ecosystem scale em-
41 ploy the first decomposer imbalance option, and use changes in CUE or
42 nutrient use efficiency to represent stoichiometric controls on respiration and
43 mineralization fluxes (Manzoni et al., 2008). However, modelling studies at
44 the pore scale have demonstrated the important effect of community adap-
45 tation and their emerging effects on element cycling (Allison and Vitousek,
46 2005; Resat et al., 2011; Wang et al., 2013). Explicit representation of com-
47 petition among several microbial groups that differ in their expression of
48 different enzymes resulted in a comparable simulated CUE across a wide
49 range of litter stoichiometry (Kaiser et al., 2014). Likely, therefore, there
50 is a need to capture the effects of community adaptation also in models at
51 ecosystem scale.

52 At least two alternatives exist to represent the effects of microbial di-
53 versity at the ecosystem scale. First, competition of several microbial pop-
54 ulations can be explicitly modelled to represent stoichiometric effects such
55 as sustained sequestration of N with high N inputs (Perveen et al., 2014).
56 Second, adaptation of effective properties of the entire microbial community,
57 such as investments into nutrient uptake (Rastetter et al., 1997; Rastetter,
58 2011) can represent the emerging effects in an abstract, but dynamic and
59 adaptive way. The adaptation of enzyme allocation was recently formalised
60 using the second imbalance strategy by the conceptual EEZY model (Moor-

head et al., 2012) and further developed using the EnzMax allocation strategy by Averill (2014). While these models show strong strategy effects on nutrient cycling at a time scale of days to months, they do not represent feedback mechanisms to the size and stoichiometry of the SOM pools, and therefore they cannot study the consequences for decadal SOM dynamics.

In this paper, we adopt the second alternative of representing microbial diversity as working hypothesis and propose a holistic scheme to represent effects of microbial adaptation of enzyme synthesis on SOM cycle at the ecosystem scale. Our aim was to tackle the need of capturing the decadal time scale effects of adaptive enzyme synthesis on SOM dynamics and nutrient recycling. We therefore extended the EEZY model to explore different consequences of alternative enzyme allocation strategies.

This paper first introduces the SEAM model (Section 2.1), a dynamical model of SOM cycling that explicitly represents microbial strategies of producing several extracellular enzyme pools (Section 2.3). Next, the effects of those strategies on SOM cycling are presented by prototypical examples (Sections 2.4 and 3.1). Finally, a calibration to an intensive pasture site (Section 2.5) demonstrates the usability of the model (Section 3.2) and compares its predictions to the ones of the SYMPHONY model (Perveen et al., 2014), which explicitly models several microbial-groups.

2. Methods

2.1. Soil Enzyme Allocation Model (SEAM)

The dynamic Soil Enzyme Allocation Model (SEAM) allows exploring consequences of enzyme allocation strategies for SOM cycling at the soil core

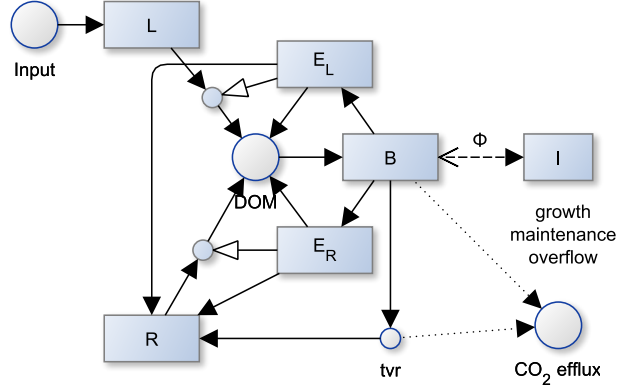


Figure 1: Model structure of SEAM: Two substrate pools (L and R) which differ in their elemental ratios are depolymerized by respective enzymes (E_L and E_R). The simple organic compounds (DOM) are taken up by the microbial community and used for synthesizing new biomass (B), new enzymes, or for catabolic respiration. Turnover of microbial biomass (tvr) is in part mineralized and the rests adds to the residue pool. Stoichiometric imbalance between DOM and B causes overflow respiration or mineralization/immobilization (Φ_B) of inorganic N (I) (further detailed in Fig. 2). Boxes correspond to pools, disks to fluxes, black arrow heads to mass fluxes, white arrow heads to other controls. Solid lines represent fluxes of both C and N, while dotted and dashed lines represent separate C or N fluxes respectively.

85 to ecosystem scale from monthly to decadal scale. The modelled system are
 86 C and N pools in SOM in a volume of soil. The system could be soil of a
 87 laboratory incubation or a layer of a soil profile, e.g. its upper 20 cm. The
 88 model represents different SOM pools containing C and N as state variables
 89 and specifies differential equations for the mass fluxes. It is driven by C and
 90 N inputs of plant litter (both above-ground and rhizodeposition), inorganic
 91 N inputs from deposition and fertilisers, as well as prescribed uptake of inor-
 92 ganic N by roots. SEAM computes output fluxes of heterotrophic respiration
 93 and leaching of inorganic N.

94 Key features are: first, the representation of several SOM pools that

Table 1: State variables and model inputs with initial values and input fluxes. Values refer to the Laqueuille pasture calibration.

Symbol	Definition	Value	Unit	Rationale
L	C in litter	571	g m^{-2}	quasi steady state
L_N	N in litter	8.15	g m^{-2}	(Perveen et al., 2014) (by their N/C ratio β)
R	C in residue substrate	10500	g m^{-2}	(Allard et al., 2007) (total stocks - L - dR)
R_N	N in residue substrate	968	g m^{-2}	by C/N ratio in (Perveen et al., 2014)
E_L	C in enzymes targeting L	0.34	g m^{-2}	quasi steady state
E_R	C in enzymes targeting R	0.20	g m^{-2}	quasi steady state
B	microbial biomass C	89.2	g m^{-2}	quasi steady state
I	inorganic N	2.09	g m^{-2}	(Perveen et al., 2014)
input_L	litter C input	969.16	$\text{g m}^{-2}\text{yr}^{-1}$	(Perveen et al., 2014) ($m_p C_p^{obs}$)
i_I	inorganic N input	22.91	$\text{g m}^2\text{yr}^{-1}$	(Perveen et al., 2014)
k_{IP}	inorganic plant N uptake	16.04	$\text{g m}^2\text{yr}^{-1}$	(Perveen et al., 2014) (assuming plant steady state: plant N export + litter N input)

95 differ by their stoichiometry, and second, the representation of enzymes that
 96 degrade specifically those SOM pools. The quality spectrum is modelled
 97 by two classes: a C rich litter pool, L , and a N rich pool that consists of
 98 microbial residues, R (Fig. 1, Table 1). The most important assumptions
 99 are described in the following paragraphs, while the symbols are explained
 100 in Tab. A.5 and detailed model equations are provided with Appendix A.

101 Decomposition of the litter and residue pools follows reverse Michaelis-
 102 Menten kinetics (Schimel and Weintraub, 2003), which is first-order to the
 103 amount of OM, and saturates with the amount of the respective enzyme.

104 C/N ratios, β , of the decomposition flux are equal to the C/N ratios of the
 105 decomposed pool. The C/N ratios of biomass and enzymes are assumed to be
 106 fixed, while those of the substrate pools may change over time due to changing
 107 C/N ratio of total influxes to these pools. Imbalances in stoichiometry of
 108 uptake and microbial requirements are compensated by overflow respiration
 109 or N mineralization. This means that if there is more C in uptake than can
 110 be used based on other constraints, such as available N, it will be respired.
 111 If there is more N in uptake than can be used by other constraints, such
 112 as available C, it will be mineralized. Total enzyme allocation is a fixed
 113 fraction, a_E , of the microbial biomass, B , per time. However, the microbial
 114 community can use different strategies to adjust their allocation to synthesis
 115 of alternative kinds of new enzymes (Section 2.3). All decomposition fluxes
 116 first fuel a pool of dissolved OM (DOM). The dynamics of this pool is usually
 117 much faster than the dynamics of the other pools. Therefore, SEAM is
 118 simplified by assuming the DOM pool to be in quasi steady state (Wutzler
 119 and Reichstein, 2013). Hence, the sum of all influxes to the DOM pool, i.e.
 120 decomposition plus part of the enzyme turnover, is taken up by the microbial
 121 community and the DOM pool is not simulated explicitly. If expenses for
 122 maintenance and enzyme synthesis cannot be met, the microbial community
 123 starves and declines in biomass.

124 *2.2. Exchange with inorganic N pools*

125 The imbalance flux, Φ_B (A.12c), lets microbes mineralise excess N, or im-
 126 mobilise required N up to a maximum rate, $u_{\text{imm,Pot}}$. The latter is assumed
 127 to increase linearly with the inorganic N pool. While this stoichiometric
 128 imbalance flux is the most widely implemented flux mechanism between mi-

129 crobial biomass and the inorganic N pools in SOM models (Manzoni and
 130 Porporato, 2009), it is not sufficient to recycle N to the inorganic pool if
 131 microbial biomass is itself N limited. Therefore, two additional mineralisa-
 132 tion fluxes are implemented in SEAM (Fig. 2). First, a fraction of microbial
 133 uptake N in DOM, Φ_u (termed uptake mineralisation), is mineralised to rep-
 134 resent the subscale imbalance flux at C-limited spots of a heterogeneous soil
 135 volume, which is in total not C-limited (Manzoni et al., 2008). Second, a
 136 fraction of microbial turnover is mineralised that accounts for grazing. Graz-
 137 ers respire a fraction of the grazed biomass C to meet their energy demand,
 138 and - assuming invariant grazer stoichiometry - must release an equivalent
 139 amount of nutrients. This mineralization component, here termed turnover
 140 mineralization Φ_{tvr} , has been formalised in the soil microbial loop hypothesis
 141 (Clarholm, 1985; Raynaud et al., 2006).

142 In the light of the introduction of these additional N mineralisation fluxes,
 143 we propose a refined term of N limitation in modelling concepts (Table 2).
 144 When microbes cannot meet their stoichiometric demand by DOM uptake
 145 but can meet their demand by immobilising inorganic N, we suggest the
 146 term *organic N limitation*. When the immobilisation flux cannot meet the
 147 stoichiometric requirement of the microbial community, we suggest the term
 148 *microbial N limitation*. Despite the maximum microbial immobilisation flux
 149 there might still be a net mineralization in the system due to uptake mineral-
 150 ization and turnover mineralization. When there is a net N immobilization
 151 in the system, i.e. a net transfer from the inorganic pool to the organic pools
 152 of SOM and microbial biomass, we suggest the term *decomposer system N*
 153 *limitation*. While the two first terms are relevant for microbial ecology, the

Table 2: Increasing levels of N limitation

Term		Definition
Organic N lim.		N in microbial uptake of organic matter is less than constrained by other elements ($\Phi_B < 0$).
Microbial N lim.		uptake of organic matter plus maximum immobilisation flux is not enough to satisfy microbial N requirements ($-\Phi_B \geq u_{\text{imm,Pot}}$).
Decomposer system N lim.		There is a net transfer from the inorganic pool to the organic pools ($\Phi = \Phi_B + \Phi_u + \Phi_{\text{tvr}} < 0$).

154 last term affects N availability for plants.

155 2.3. Enzyme allocation strategies

156 Microbes in SEAM allocate a proportion α of their total enzyme invest-
157 ments, $a_e B$, to the synthesis of enzymes, syn_E , targeting the N-rich R sub-
158 strate and a proportion $1 - \alpha$ to the synthesis of enzymes targeting the
159 N-poor, but better degradable L substrate.

$$\text{syn}_{E_R} / (\text{syn}_{E_R} + \text{syn}_{E_L}) \equiv \alpha \quad (1)$$

160 Four different strategies of allocating investments among synthesis of al-
161 ternative enzymes were explored in this study (Table 3).

162 The **Fixed** strategy assumes that allocation is independent of, and not

Table 3: Microbial enzyme allocation strategies

Strategy	Allocation is
Fixed	independent, constant
Match	adjusted to achieve balanced growth, i.e. β_{DOM} matches microbial demands
EnzMax	equal to Match-Allocation if microbial N-limited, and equal to $\alpha = 0.5$ otherwise
Revenue	proportional to return per investments into enzymes

163 changing with changes in substrate availability.

$$\alpha = \text{const.} = 1/2 \quad (2)$$

164 This strategy corresponds to the models without enzyme allocation adapta-
 165 tion where decomposition rate is a function of microbial biomass (Wutzler
 166 and Reichstein, 2008).

167 The **Match** strategy assumes that microbes regulate enzyme synthesis
 168 in a way that the decomposition products balance their stoichiometric de-
 169 mands (Moorhead et al., 2012). The partitioning coefficient α is derived by
 170 equating the C/N ratio of the sum of uptake fluxes after other expenses,
 171 such as growth and maintenance respiration, to the C/N ratio of microbial
 172 biomass, β_B (3). The equation of (Moorhead et al., 2012) has been adapted
 173 to take into account inorganic N immobilization and splitting their CUE
 174 into growth respiration and an "anabolic" microbial efficiency accounting for
 175 growth respiration.

$$\beta_B = \frac{\epsilon(\text{dec}_L + \text{dec}_R - r_M)}{\text{dec}_L/\beta_L + \text{dec}_R/\beta_R - \Phi_M}, \quad (3)$$

176 where dec_L , and dec_R are depolymerisation fluxes of the litter and residue
 177 pools, respectively (A.4), which both are a function of enzyme levels and,
 178 hence, indirectly a function of α . r_M is maintenance respiration (A.2b), ϵ is
 179 the anabolic microbial efficiency accounting for growth respiration (A.7), β_i
 180 are C/N ratios of the respective pools i , and Φ_M is the net flux of N from
 181 living microbes to the mineral N pool. Equation 3 for simplicity neglects the
 182 small inputs of enzymes to DOM. Here, we assume that microbes use the
 183 maximal immobilisation of inorganic N, $u_{\text{imm,Pot}}$ (A.9) to meet their stoichio-
 184 metric requirements with the Match strategy. Hence, the net N imbalance
 185 flux is the difference between mineralization during uptake and the immobili-
 186 sation: $\Phi_M = \Phi_u - u_{\text{imm,Pot}}$. With microbial N limitation, (3) has no solution.
 187 In this case, the enzyme effort is allocated entirely to the N-rich substrate
 188 ($\alpha = 1$), and excess carbon uptake is respired by overflow respiration.

189 If current enzyme pools E_S , are assumed to be in quasi steady-state with
 190 their respective substrate $S \in \{L, R\}$ and microbial biomass, then equation
 191 3 can be solved for the partitioning coefficient, α .

$$\alpha_M = f_{\alpha\text{Fix}}(L, \beta_L, R, \beta_R, E_L, E_R, r_M, \Phi_M) \quad (4a)$$

$$\alpha = \begin{cases} 0, & \text{if } \alpha_M \leq 0 \\ 1, & \text{if } \alpha_M \geq 1 \\ \alpha_M, & \text{otherwise} \end{cases} \quad (4b)$$

192 where the long equation (4a) is given with supplementary material together
 193 with R-code and the SYMPY script of its derivation. The bound to one is
 194 necessary to handle the case of microbial N limitation. The bound to zero
 195 corresponds to the theoretical case where the C-rich substrate may not suffice
 196 to cover microbial C demands relative to N demands.

197 The **EnzMax** strategy (Averill, 2014) matches stoichiometry if microbes
 198 are substrate N limited, and uses a fixed allocation coefficient $\alpha = 0.5$ if
 199 microbes are not substrate N-limited, i.e. C-limited. In order to avoid frequent
 200 jumps between the two cases, a weighted mean between the two fluxes was
 201 used for N imbalance fluxes near $\Phi_B = 0$ with α approaching the match
 202 solution (4a) for N mineralization or approaching 0.5 for N immobilization
 203 indicating C limitation.

204 The **Revenue** strategy assumes that the microbial community adapts in
 205 a way to ensure that the investment into enzyme synthesis is proportional to
 206 its revenue, i.e. the return per investment regarding the currently limiting
 207 element:

$$\alpha_C = \frac{\text{rev}_{RC}}{\text{rev}_{LC} + \text{rev}_{RC}} \quad (5a)$$

$$\alpha_N = \frac{\text{rev}_{RN}}{\text{rev}_{LN} + \text{rev}_{RN}}, \quad (5b)$$

208 where rev_S is the revenue from given substrate $S \in \{L, R\}$ with microbial
 209 C and N limitation respectively. The revenue is computed on the current
 210 status quo, i.e. the current enzyme levels. Appendix B explains why invest-
 211 ing proportional into all enzymes is better than investing into the single best

enzyme. The return is the current decomposition flux from the substrate de-
graded by the respective enzyme (A.4), and the assumed investment balances
enzyme turnover to keep current enzyme levels, E_S^* (A.3).

$$\text{rev}_{SC} = \frac{\text{return}}{\text{investment}} = \frac{\text{dec}_{S,Pot} \frac{E_S^*}{K_{M,S} + E_S^*}}{k_E E_S^*} = \frac{\text{dec}_{S,Pot}}{k_E (K_{M,S} + E_S^*)} \quad (6a)$$

$$\text{rev}_{SN} = \frac{\text{dec}_{S,Pot} \frac{E_S^*}{K_{M,S} + E_S^*} / \beta_S}{k_E E_S^* / \beta_E} = \text{rev}_{SC} \frac{\beta_E}{\beta_S}, \quad (6b)$$

where k_E is rate of enzyme turnover, $K_{M,S}$ is the enzyme's substrate affinity,
 $\text{dec}_{S,Pot}$ is enzyme saturated decomposition flux (A.4), and β are C/N ratios
of the respective pools.

There are two resulting partitioning coefficients, α_C and α_N with C or
N-limited microbial biomass, respectively. In order to avoid frequent large
jumps under near co-limitation, SEAM implements a smooth transition be-
tween these two cases as a weighted average.

$$\alpha = \frac{w_{CLim} \alpha_C + w_{NLim} \alpha_N}{w_{CLim} + w_{NLim}}, \quad (7)$$

where w is the strength of the limitation of the respective element, specifically
the ratio of required to available biomass synthesis fluxes (A.13).

2.4. Prototypical simulation experiments

Several prototypical simulation experiments (Table 4) were used to ex-
plore the consequences of the different microbial enzyme allocation strategies
(2.3) for the simulated SOM dynamics. They increase in complexity from
a soil incubation experiment to a decadal CO₂ manipulation treatment. All

Table 4: Prototypical simulation experiments

Experiment	Explored issue
VarN-Incubation	Efficiency of using given fixed substrate levels that vary by N content
Substrate-feedback	Possibility and size of steady state substrate pools
Priming	Increased substrate decomposition and mineralization after a pulse addition of fresh litter
CO ₂ -Fertilization	N mineralization with a continued input of increased litter C but constant litter N inputs

experiments used parameter values given in Table A.5 unless stated otherwise in this section. For the prototypical experiments, the inorganic N pool was kept constant at $I = 0.4 \text{ gN m}^{-2}$, while inorganic N feedbacks were considered in Section 2.5.

The **VarN-Incubation** experiment explored how efficiently substrates of a given stoichiometry were used for microbial biomass growth with the different enzyme allocation strategies. A simplified model version was employed in this experiment, where all the inputs and feedback to the substrate pools (L and R) were neglected, and in which these pools were kept constant ($dL/dt = dR/dt = 0$). This simplification led to a quasi steady state of microbial biomass and enzyme levels for the given substrate supply. This experiment mimics a short-term incubation experiment, where changes in litter and residue pools are negligible small. The assumed boundary condi-

242 tions for this experiment were fixed substrate carbon of $L = 100 \text{ gC m}^{-2}$, and
243 $R = 400 \text{ gC m}^{-2}$. The C/N ratio of the residue pool was assumed constant at
244 $\beta_R = 7$, whereas litter C/N ratio varied between 18 and 42 ($\beta_L = [18, \dots, 42]$).

245 The **Substrate-feedback** experiment explored the decadal trajectories
246 of the entire system including feedback to the substrate pools. Litter input
247 was assumed constant at a rate of $\text{input}_L = 400 \text{ gC m}^{-2}\text{yr}^{-1}$ with a C/N
248 ratio of $\beta_{\text{input}_L} = 30$.

249 The **Priming** experiment explored the effect of rhizosphere priming, i.e.
250 the input of fresh litter into a volume of subsoil that is newly explored by
251 a root. Specifically, the simulations evaluated the fluxes after an addition
252 of 50 gC m^{-2} and a respective amount of N (C/N ratio $\beta_{\text{input}_L} = 30$) on
253 a soil that otherwise received a litter input of only $30 \text{ gC m}^{-2}\text{yr}^{-1}$ (and
254 respective N with $\beta_{\text{input}_L} = 30$) for a decade. The assumption is made that
255 the rhizodeposition litter input (both pulse and continuous) was very easily
256 degradable litter, specifically with a maximum turnover of $k_L = 10 \text{ day}^{-1}$.
257 The amendment of rhizodeposition was simulated by a single pulse, i.e. a
258 step change in the litter pool.

259 The **CO₂-Fertilization** experiment explored the effect of increased con-
260 tinuous litter C input, which is expected with elevated atmospheric CO₂
261 concentration. The simulations started from steady state corresponding to
262 initial litter C input of $\text{input}_L = 400 \text{ gC m}^{-2}\text{yr}^{-1}$, applied 20% increased C
263 inputs during years 10 to 60, and applied initial litter inputs again during the
264 next 50 years. The litter N inputs were kept constant over time, implying
265 an increase in the litter C/N ratio of 20%. Litter input rate was assumed
266 constant across the year.

267 *2.5. Calibration to a fertilised pasture site*

268 To test the capacity of SEAM to simulate the net carbon storage of a
269 pasture site including feedback of the inorganic N pool, we calibrated the
270 model to data of an intensive pasture. The intensive pasture calibration was
271 tackled only with the Revenue strategy, because the Match and the EnzMax
272 strategies had already shown inadequate for scenarios including feedbacks to
273 substrate pools during in the Substrate-feedback experiment. The control
274 case of the Fixed strategy did not allow for adaptation of microbial enzyme
275 allocation.

276 The model drivers and most of the parametrisation and drivers (Tables
277 A.5 and 1) were taken from Perveen et al. (2014). The site is a temperate
278 permanent pasture located at an altitude of 1040m a.s.l. in France (Laque-
279 uille, 45°38'N, 2°44'E), receives an annual precipitation of 1200 mm and has
280 an annual mean temperature of 7 °C.

281 The N-balance of the fertilised pasture is characterised by very high N-
282 inputs. A fraction of this N is sequestered in accumulating SOM, a fraction
283 is lost to leaching, while the remainder is exported with plant biomass har-
284 vest. Plant uptake of inorganic N was computed as the sum of plant litter
285 production and plant biomass exports, keeping the plant N pool constant.

286 Model parameters were chosen corresponding to Table 1 in Perveen et al.
287 (2014), and initial litter and SOM pools were prescribed to observed val-
288 ues. Three parameters were calibrated: the maximum decomposition rates
289 of substrate pools, k_L and k_R , and the anabolic carbon-use efficiency, ϵ . Ini-
290 tial pools of microbial biomass and enzymes were set to the decadal steady
291 state in order to prevent large transient initial fluctuations in model pools.

292 The calibration used the *optim* function from R *stats* package (R Core Team,
293 2016) and minimised the differences between model predictions and observa-
294 tions normalised by the standard deviation of the observations. The calibra-
295 tion used observations of the litter OM, the inorganic N, leaching, and rate
296 of change of the total SOM pool ($\approx dR/dt$ if L is near quasi steady state).

297 Subsequently, the calibrated parameters were used to generate predictions
298 for several scenarios of altered inputs to the system.

299 The R-code to generate the results and figures of this paper is available
300 upon request.

301 3. Results

302 First, the results of several prototypical artificial simulation experiments
303 clarify the general behaviour and features of the SEAM model. Next, results
304 of a parameter calibration demonstrate the model’s ability to simulate the
305 observed C and N dynamics of an intensive pasture and explore feedbacks
306 with the dynamics of the inorganic N pool.

307 3.1. Prototypical simulation experiments

308 Under the **VarN-Incubation** experiment, in which the substrate pools
309 were fixed, there were marked differences in the effect of allocation strategies
310 on simulated biomass and the imbalance flux (Fig. 3).

311 The Match strategy allowed balanced growth, and yielded the highest
312 substrate efficiency and lowest mineralization fluxes among the enzyme allo-
313 cation strategies. Across a range of litter C/N ratios of 22 to 42 the Match
314 strategy yielded non-positive imbalance fluxes, i.e. no mineralization of ex-
315 cess N or overflow respiration of excess C. This means, that microbes could

316 utilize all food taken up for productive expenditures. However, the match
317 strategy also yielded lowest biomass among the strategies. In the discussion
318 we argue that this means an inferior strategy.

319 With the Revenue strategy, enzyme allocation α also varied with litter N
320 content, but to a lesser extent. With litter containing enough N (low C/N
321 ratio), still about 5% of the enzyme synthesis C expenditures were allocated
322 into R-degrading enzymes. With high C/N ratio of litter, investment into R-
323 degrading enzymes increased to about 30%, much less than with the Match
324 strategy. Hence, the Revenue strategy yielded higher overflow respiration
325 associated with a low carbon-use efficiency (CUE). However, it gained more
326 of the limiting element N with the decomposition flux and supported higher
327 microbial biomass.

328 The Fixed strategy yielded higher N-mineralization due to larger stoi-
329 chiometric imbalance at low C/N ratios. At high C/N ratios its constant
330 allocation coefficient was intermediate between the other strategies, leading
331 to intermediate values of all the other outputs.

332 The EnzMax strategy yielded predictions that were equal to the Match
333 strategy with low C/N ratios, and equal to the Fixed strategy with high C/N
334 ratios, and a transition between those two at C/N ratios around 23.

335 When the substrate pools were allowed to be refuelled by microbial and
336 enzyme turnover with the **Substrate-feedback** experiment, both Fixed and
337 the Revenue strategies caused substrate pools to approach a steady state.
338 However, the microbes with Match strategy solely degraded the stoichiomet-
339 rically better matching N-rich residue pool, R . Hence, they declined together
340 with the residue pool despite the large amount of N accumulating in the stoi-

341 chio metrically less favourable litter pool, L , (Fig. 4). Similarly, with EnzMax
342 strategy the litter pool accumulated until microbes became C limited. Then
343 there was an unreasonable explosion like increase of microbial biomass, un-
344 til the accumulated litter pool had been degraded. Because of the Match
345 and the EnzMax strategies yielded unreasonable behaviour when including
346 feedback to substrate pools in the model, they were omitted in the following
347 simulation experiments.

348 When the soil was amended with a pulse of litter with the **Priming**
349 **experiment**, a clear true priming effect, i.e. an increased decomposition
350 of the existing SOM, was simulated with the Fixed and Revenue strategy.
351 The priming effect occurred due to a strong enhancement of residue decom-
352 position (Fig. 5 top). This enhancement was stronger with the Revenue
353 strategy than with the Fixed strategy, primarily because of a higher sim-
354 ulated microbial biomass with the Revenue strategy. In consequence, also
355 the N-mineralization flux due to microbial turnover was larger with the Rev-
356 enue strategy (Fig. 5 bottom). Note, that the time scale of the simulated
357 priming effect of more than 100 days was longer than observed in priming
358 experiments.

359 When the continuous litter C input was assumed to be higher for 50
360 years with the **CO₂-fertilisation experiment**, enzyme allocation strategies
361 yielded marked difference in SOM stocks (Fig. 6) and nutrient recycling
362 (Fig. 7). While litter stock, L , increased with both strategies following
363 the increased input, the residue stock, R , slightly increased with the Fixed
364 strategy, but declined strongly with the Revenue strategy. This was the con-
365 sequence of an increased mining of the R pool with the Revenue strategy.

366 Accordingly, N mineralization was much stronger with the Revenue strategy
367 during the elevated CO₂ period, with the largest contribution from mineral-
368 ization by microbial turnover.

369 In this experiment the initial N immobilization flux was sufficient to avoid
370 microbial N limitation ($-\Phi_B < u_{immo,Pot}$). The increased C-inputs during
371 the period of elevated CO₂ then shifted the system to microbial N limitation,
372 where required N immobilization was larger than the maximum immobiliza-
373 tion flux. The adaptive Revenue strategy in effect helped plants to liberate
374 more N from the SOM under elevated CO₂ in the following way. There
375 was a net transfer from SOM R pool to living biomass and subsequently to
376 microbial turnover that was in part mineralized. The mineralization of the
377 turnover of the increased microbial biomass returned more N to the mineral
378 N pool than was taken up by the immobilization flux of living microbes.
379 The increased mineral N pool then could be utilized by plants. However,
380 this response was transient. After litter inputs returned to initial values, the
381 system recovered towards the initial state but only on centennial time scale
382 that would even be longer if prescribing a longer turnover time for slower
383 SOM pools.

384 3.2. *Intensive pasture simulation*

385 The calibrated SEAM model successfully simulated the observed C and
386 N balance of the Laqueuille intensive pasture (Figure 8). In contrast to the
387 prototypical simulation experiments, here, the feedback of the inorganic N
388 pool was included, the model was driven and compared to observed values,
389 and only the Revenue strategy has been considered.

390 The observed continuous build-up of an organic N pool in the residue

391 SOM was driven by the system's positive N balance. Two pathways caused
392 the model behaviour in SEAM. First, inorganic N was taken up by the plant
393 and returned to the soil via organic N in litter. Second, microbial biomass
394 immobilised inorganic N due to its stoichiometric imbalance with the sub-
395 strate. The microbial biomass was N-limited when only considering uptake
396 of organic substrate. However, it was C-limited when accounting for immo-
397 bilisation of inorganic N (Table 2).

398 Simulated alteration of C and N inputs to the system strongly affected the
399 internal SOM and nutrient cycling. Effects were shown by several simulation
400 scenarios that started from the calibrated state but applied a step change in
401 inputs of litter or inorganic N (Figure 9) as detailed in following paragraphs.

402 Increased litter C input by 50% together with an increased litter C/N
403 ratio by 25% (elevated CO₂ scenario) caused a shift in enzyme allocation
404 towards enzymes degrading the N-rich residue pool and an increase of the
405 litter pool. The higher input also increased the mineral N demand of both
406 the plant to balance increased biomass synthesis and the microbial biomass
407 with its higher stoichiometric imbalance. The resulting decrease in mineral N
408 also decreased leaching losses. Moreover, ecosystem available N was re-used
409 more often, because of a higher turnover flux of N in increased microbial
410 biomass.

411 Decreased inorganic N inputs from 22.9 g m⁻²yr⁻¹ down to 1 g m⁻²yr⁻¹
412 together with a doubling of litter C/N ratio caused a strong shift in enzyme
413 allocation towards enzymes degrading the N-rich residue SOM with similar
414 consequences as with increased C input, such as an increase in litter OM.
415 However, in this scenario, the decreased N inputs caused a depletion of the

416 mineral N pool. As a consequence, the microbial biomass could not use
417 immobilisation to balance substrate stoichiometry and became microbially
418 N-limited. This caused overflow respiration and a decreasing trend in residue
419 SOM.

420 Increased inorganic N inputs from $22.9 \text{ g m}^{-2}\text{yr}^{-1}$ up to $25.6 \text{ g m}^{-2}\text{yr}^{-1}$
421 together with a decrease of litter C/N by 25% did not much affect the sys-
422 tem behaviour, because the soil system was already C-limited before. The
423 microbial biomass could only immobilise a small fraction of the additional
424 N to build up new SOM. Instead, N accumulated in the inorganic pool with
425 associated increased losses to leaching.

426 4. Discussion

427 Microbial adaptation of enzyme synthesis to substrate availability ben-
428 efited the community so that higher microbial biomass levels could be sus-
429 tained on a wider range of substrate stoichiometry. The different prototypic
430 simulation experiments and the simulation of the intensive pasture led to
431 similar conclusions on the effects of adaptation of enzyme allocation.

432 4.1. Amounts of substrates matter

433 The amount of substrate and the substrate stoichiometry are both im-
434 portant for regulating enzyme allocation. The Match strategy failed to ac-
435 count for substrate amount, assuming that microbes adapt to achieve bal-
436 anced growth under a wide range of substrate stoichiometry (Moorhead et al.,
437 2012; Ballantyne and Billings, 2014). This strategy yielded lower microbial
438 biomass both in the VarN-Incubation (Fig. 3) and in the Substrate-feedback

439 experiments (Fig. 4). We argue that producing less biomass means an in-
440 ferior strategy, because slower growing microbes have a competitive disad-
441 vantage to faster growing microbes that have otherwise same properties such
442 as maintenance requirements. Match-strategy microbes focused on degrad-
443 ing a stoichiometrically balanced, but declining residues pool, leaving the
444 large amount of N available in a stoichiometrically less favourable litter pool
445 untouched (Fig. 4).

446 The study of Averill (2014) also found that the best microbial allocation
447 strategy maximised growth instead of C or N use efficiency. It found that
448 with C limitation the best allocation would be strictly equal to all the en-
449 zymes. However, the study did not yet consider feedbacks to the substrate
450 pools, nor immobilization of inorganic N. Moreover, it used a decomposi-
451 tion equation that was completely independent of the amount of available
452 substrate. The proposed EnzMax strategy would allocate the same amount
453 of resources to enzymes that depolymerize a tiny substrate pool as to en-
454 zymes that depolymerize a large substrate pool. The EnzMax strategy was
455 implemented in this study with a different decomposition equation (A.4).
456 This combination led to unreasonable behaviour in the Substrate-feedback
457 experiment. During N limitation a large litter pool was built up, and after
458 microbes became C limited they grew explosive-like to unreasonable high
459 values until the accumulated amount of litter had been degraded (Fig. 4).

460 These findings imply that microbial enzyme allocation strategies should
461 account for substrate amounts.

462 4.2. *Community adaptation leads to a more efficient substrate usage*

463 The adaptive Revenue strategy consistently supported higher biomass
464 and had lower N mineralization fluxes at steady state compared to the non-
465 adaptive Fixed strategy with the VarN-Incubation experiment (Fig. 3). Sim-
466 ilar patterns appeared with the other experiments (Figs. 4 and 7). Such
467 better substrate usage is in line with results of individual based small-scale
468 modelling (Kaiser et al., 2014). The finding implies that N mineralization
469 fluxes with imbalanced substrates may be lower than inferred from previous
470 modelling studies that did not account for community adaptation.

471 4.3. *Comparison to observed changes in enzyme stoichiometry*

472 The SEAM model focuses on community adaptation of enzyme synthesis.
473 It predicts a change in the ratio of enzyme activities of enzymes degrading
474 C-rich plant litter versus enzymes degrading the N-rich residue SOM when
475 changing inputs of N to the soil. While only low variation in stoichiometry of
476 N-degrading versus C-degrading enzymatic activity is observed across biomes
477 (Sinsabaugh et al., 2009), microcosm studies detect short-term changes of
478 enzyme activities with N fertilization (Kumar et al., 2016), but their obser-
479 vations differ between different kinds of N-degrading enzymes. Hence, the
480 evidence is mixed.

481 SEAM also predicts accelerated turnover of the residue pool associated
482 with increased enzyme activity of N-rich R-pool degrading enzymes after in-
483 creased inputs of litter C in relation to litter N. Such patterns are observed
484 at field scale at Duke forest, where Phillips et al. (2011) found an increased
485 activity of extracellular enzymes involved in breakdown of organic N asso-
486 ciated with accelerated SOM turnover after increased root exudation with

487 elevated CO₂. In an artificial root exudation experiments at the same site,
488 Drake et al. (2013) found an increase of N degrading NAG enzyme activity
489 with C-only inputs and a shift from oxidative towards hydrolytic enzymes
490 decomposing low molecular weight (lmw) components inputs that contained
491 both C and N. Assuming that the lmw-components have higher C/N ratios,
492 this observed shift is in line with SEAM predictions.

493 4.4. *SOM as nutrient bank*

494 Nitrogen was stored in residue SOM during periods of high N inputs and
495 released during periods of low N inputs relative to C inputs in simulations
496 (Fig. 6). When there was excess litter C, the microbial community prefer-
497 entially depolymerised, or mined, the N-rich residue pool, and thereby made
498 the N available for plants. When carbon inputs were low, microbes degraded
499 the residue pool to a lesser extent, but continued to build new residue via
500 microbial turnover. Hence, under low C conditions, the microbes kept N in
501 the decomposer system instead of releasing it through mineralisation.

502 This 'bank' mechanism (sensu Perveen et al., 2014) also worked when
503 simulating the intensive pasture (Fig. 9). During simulations of high inor-
504 ganic N inputs, N was sequestered in SOM at a high rate. With decreased
505 inorganic N inputs, the sequestration rate decreased until it became negative,
506 that is the N in slower decomposing SOM pools was mined. In the long-term,
507 i.e. centuries, the inputs to the system have to balance the outputs of the
508 system. Hence, in the intensive pasture simulation, inorganic N pools and
509 N leaching increased with the increase of SOM with the SEAM model. The
510 conservation or release of N by the bank mechanism implies greater potential
511 for ecosystems to avoid progressive N limitation (Norby et al., 2010; Franklin

et al., 2014; Averill et al., 2015). This finding potentially has consequences on feedbacks of global change, especially on the projected C land uptake (Friedlingstein et al., 2014).

4.5. *Priming effects liberate N*

Priming effects, i.e. the altered decomposition of SOM after soil amendments (Kuzyakov et al., 2000), are a potential mechanism to help plants stimulate N release from the SOM for plant nutrition. Priming effects and associated increased N mineralization were simulated for both, the Fixed and Revenue strategies (Fig. 5). With adaptive microbial enzyme allocation (Revenue strategy), increasing plant litter input or increases in litter C/N upregulated the decomposition of the N-rich residue pool (Fig. 6). This in turn influenced the distribution of N in the ecosystem, and N availability for plants (Fig. 7). This active role of plant inputs has been demonstrated in a soil incubation experiment (Fontaine et al., 2011) and has been further conceptualised with the SYMPHONY model (Perveen et al., 2014). Our results are in line with these studies, although our explanation is on a more abstract level (see Section 4.7).

Mineralization of microbial turnover was necessary in SEAM to allow liberation of N by priming effects. Without sufficient microbial turnover mineralization, changes in litter inputs could not shift the system to microbial N limitation in additional simulation experiments (Appendix C). These findings corroborate the need for representing the effects of soil heterogeneity (Manzoni et al., 2008) and microbial turnover by grazing (Clarholm, 1985; Raynaud et al., 2006) for making N available for plants under N limitation.

536 *4.6. Mismatch in time scale of priming effects*

537 The unrealistically long time-scale of the priming effect of several months
538 in SEAM (Fig. 5) resulted from both, the long turnover time of enzymes,
539 and the sustaining positive feedback between amounts of microbial biomass
540 and enzymes. It was in contrast with incubation studies that observe priming
541 effects within days or weeks that rapidly declined after the amendment has
542 been used up (Blagodatskaya et al., 2014). The priming timescale in SEAM
543 was longer than the duration of the uptake pulse of the *L* amendment that
544 only lasted a few days. It was controlled by simulated lifetime of enzymes
545 and enzyme turnover, which SEAM described as first order kinetics with a
546 turnover of about a week. Moreover, the priming timescale was prolonged by
547 the positive feedback of increased microbial biomass producing more enzymes
548 that again fuelled microbial biomass.

549 One possible hypothesis for a shorter priming time-scale is a different dy-
550 namics of enzyme turnover. However, prescribing a shorter turnover time of
551 enzymes would require an unrealistically large effort of producing enzymes by
552 microbial biomass. More sophisticated models of different enzyme turnover
553 kinetics including stabilisation of a part of the enzymes on mineral surfaces
554 (Burns et al., 2013) may be able to resolve such contradictions. Testing this
555 hypothesis would require observations of the fraction of C uptake allocated
556 to enzyme synthesis and on age distribution of enzymes in the soil which
557 might be feasible with labelling studies.

558 An alternative cause for a shorter priming time-scale may be an important
559 control of enzyme activity that is not as strongly coupled to microbial biomass
560 dynamics. Some enzymes such as peroxidase need to be fuelled by labile OM

561 themselves (Rousk et al., 2014) with no immediate relationship to microbial
562 biomass dynamics. This explanation, however, implies that enzyme activity
563 and decomposition of SOM become largely decoupled from enzyme synthesis
564 and microbial dynamics in the short-term. This option is contrary to the
565 assumption of most current models that simulate the priming effect. Such
566 a fundamental change of model assumption would affect most implications
567 gained from SOM modelling studies that involve soil microbes.

568 Another cause for a shorter priming time-scale, is a diminished sustaining
569 positive feedback between enzymes and microbial biomass. Currently, graz-
570 ing is modelled as an implicit part of a first-order microbial turnover. With
571 increasing microbial biomass, grazers become more efficient (Clarholm, 1981).
572 With implementing a time-lagged stronger increase in microbial turnover rate
573 with microbial biomass, biomass levels would decrease faster to pre-treatment
574 levels and help to shorten the time-scale of the priming effect. Testing this
575 hypothesis requires data on grazing during priming effects.

576 Overall, the mismatch in the time scale of priming between simulations
577 and observations hints to gaps in understanding of short-term SOM turnover.
578 However, this model limitation does not impair the simulated longer-term
579 microbial community controls on SOM cycling both in the prototypic simu-
580 lation and at the pasture site. We argue therefore that the simulated decadal
581 patterns are robust, because they are more strongly controlled by the pro-
582 portions in enzyme synthesis than by the time scale of priming effects.

583 *4.7. A holistic view for upscaling*

584 The presented SEAM model takes a holistic view (Panikov, 2010) of mi-
585 crobial community and their adaptations instead of explicitly describing mi-

586 crobial diversity. In this respect, it differs from the SYMPHONY model
587 (Perveen et al., 2014) and similar models (Fontaine et al., 2003), which ex-
588 plicitly model several microbial groups. However, the effective behaviour of
589 the presented SEAM model is similar to these models. SEAM assumes that
590 community composition adapts to external drivers. Specifically, SEAM de-
591 scribes an adaptive allocation of resources into depolymerisation of different
592 substrates by assuming that the community composition reacts to changed
593 substrate availability in a way to balance microbe’s revenue of the currently
594 limiting element. While the mechanistic approach of the SYMPHONY model
595 explicitly represents this adaptation by shifts between microbial groups, the
596 holistic approach represents its effects at community level. While the mecha-
597 nistic approach provides more detailed understanding, the proposed abstrac-
598 tion of microbial competition is a step forward to better represent couplings
599 of soil carbon and nutrient cycles in large-scale ecosystem models, as it ob-
600 viates the need to correctly parameterise the underlying details of several
601 microbial guilds.

602 The holistic SEAM model yielded qualitatively similar predictions as the
603 mechanistic SYMPHONY model with simulating priming effects, the bank
604 mechanism, and a continuous SOM sequestration under high inorganic N in-
605 puts. SEAM differed from SYMPHONY in the prediction of the inorganic
606 N pool during low N inputs. Specifically, SEAM predicted a decrease in this
607 pool, while SYMPHONY predicted an increase in this pool due to changed
608 competition (Perveen et al., 2014). The difference is probably caused by dif-
609 ferent assumptions on how the DOM pool is shared among groups of the mi-
610 crobial community and resulting different competition conditions. In SEAM,

decomposition products become mixed in a shared DOM pool, while in the SYMPHONY model the decomposition products are not shared between the microbial groups. The truth at pore scale is in between, in that decomposition products are mainly used by the group that is producing the extracellular enzymes, while a part of the DOM diffuses also to other groups (Kaiser et al., 2014). At larger scales, such details cannot be measured or resolved. The difference in model prediction implies that the rationality of the simplified model assumptions of a mixed DOM pool can be qualitatively tested against observations.

4.8. Testable predictions of change of SOM C/N ratios

The SEAM model can be used to predict decadal patterns of SOM cycling following changes in substrate stoichiometry. Observations of such patterns provide evidence for or against the modelling assumptions. Specifically, SEAM predicted a change in proportions of the litter pool and the SOM pool (Fig. 6). While these abstract pools are not directly comparable to observations, a measurable consequence is the associated change of total SOM C/N ratio at the time scale of turnover of the residue pool. Specifically, SEAM predicted a decline in SOM stocks and an increase of SOM C/N with FACE experiments at formerly C-limited systems over time scales of several decades. Observed accelerated SOM turnover at the Duke forest after 12 years of elevated CO₂ (Drake et al., 2011) is a first indication, although there is a continuum of responses to experimental CO₂ increase across sites.

633 4.9. Outlook

634 The biggest limitation of the SEAM model is its focus on a single process:
635 community adaptation of enzyme allocation. In order to focus, we had to
636 ignore several other important processes. One such process is the second mi-
637 crobial community strategy of handling substrate stoichiometric imbalance,
638 the adaption of stoichiometry of microbial biomass. Although the poten-
639 tial of this biomass adaptation is thought to be quite limited (Mooshammer
640 et al., 2014b), it will need to be tested whether these two strategies can be
641 combined within a model.

642 Next, the optimality principle will be extended to also determine the pro-
643 portion of uptake that is allocated to enzyme synthesis. Presence of cheaters,
644 i.e. microbes that consume substrate but without producing enzymes, effec-
645 tively lower the community-level allocation to enzymes (Kaiser et al., 2014).
646 We could assume that community development maximizes biomass produc-
647 tion. Such an assumption can be used to compute the optimal community
648 enzyme synthesis and allows exploring effects on SOM cycling, such as more
649 constrained carbon and nutrient use efficiencies.

650 Moreover, SEAM will be simplified by assuming quasi-steady state of
651 biomass or enzyme pools (Wutzler and Reichstein, 2013). These simplifi-
652 cations will lead to fewer parameters and improved parameter identifiability
653 in model calibration to observations (Xu et al., 2014). Together with im-
654 plementing the influence of environmental factors such as temperature and
655 moisture (Davidson et al., 2012), these changes will make SEAM more suit-
656 able to be used as a component within larger scale land surface models.

657 5. Conclusions

658 The SEAM model (Fig. 1) provides a holistic description of community
659 adaptations. It yields qualitatively similar predictions as microbial-group-
660 explicit models with the ability to represent priming effects, bank mechanism,
661 and a continuous SOM sequestration with high inorganic N inputs (Fig. 9).
662 Hence, this study is an important step for providing an abstract description
663 of microbial community effects and adaptations, with the long-term goal of
664 including the important mechanisms into earth system models.

665 Adapting the allocation of resources into the synthesis of different en-
666 zymes can be an effective means of the microbial community to react to
667 changing substrate stoichiometry. Allocation adaptation strategies helped
668 the simulated microbial biomass in SEAM to grow larger across a wider
669 range of substrate stoichiometry (Fig. 3). Among the tested strategies, the
670 Revenue strategy, which accounts for the amount of substrate pools and their
671 stoichiometry, was particularly successful. These findings imply that models
672 simulating soil carbon and nutrients dynamics (Fig. 5) need to account for
673 adaptations in carbon and nutrient strategies. Accounting for adaptations
674 will be especially important when studying the competition for nutrients
675 between soil microorganisms and plants, because SOM can function as a
676 storage to sequester surplus nutrients and prevent them from being lost from
677 the system (Fig. 6 and 7).

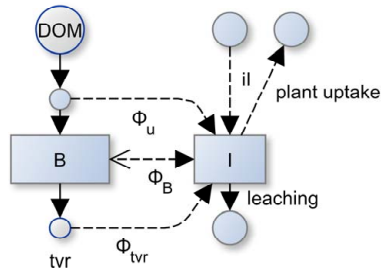


Figure 2: Total mineralization flux in SEAM sums three components: $\Phi = \Phi_u + \Phi_B + \Phi_{tvr}$. In addition to the maybe negative imbalance flux, Φ_B of microbial biomass, B , there are two additional mineralization fluxes feeding the inorganic pool, I : first, mineralization during uptake, Φ_u , and second, mineralization during microbial turnover, Φ_{tvr} . The N dynamics depends also on fluxes across the system boundary, namely input of organic N with litter, input of inorganic N, iI , leaching, and plant uptake of inorganic N.

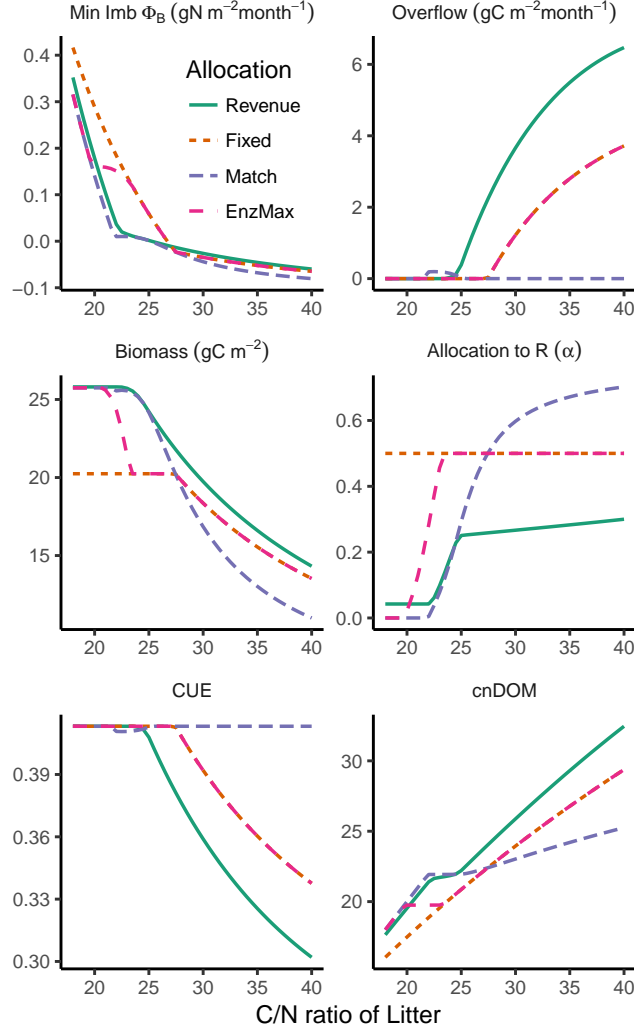


Figure 3: VarN-Incubation experiment: The match enzyme allocations strategy yielded highest resource efficiency, i.e. lowest mineralization fluxes (negative or small N mineralization and at the same time no C overflow respiration) across a large range of C/N ratios. Microbes with alternative strategies, however, were more competitive as indicated by a higher biomass. The patterns are caused by different adaptation of resource allocation (α) affecting C/N ratio of the decomposition flux (cnDOM) and carbon use efficiency (CUE).

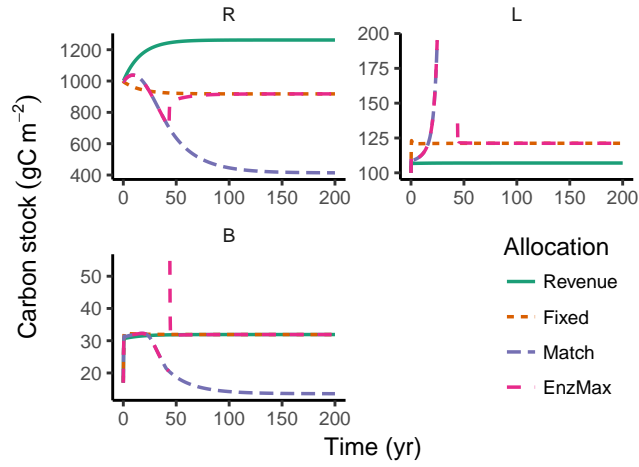


Figure 4: Substrate-feedback experiment: The match strategy was not viable when considering feedback to substrate pools. Microbes with the Match-strategy degraded the stoichiometrically matching but declining R substrate pool and their biomass, B, declined despite the large N stores in stoichiometrically less favourable litter, L. Note that the range of B and L has been limited and does not display the unreasonably large values with the Match and EnzMax strategies.

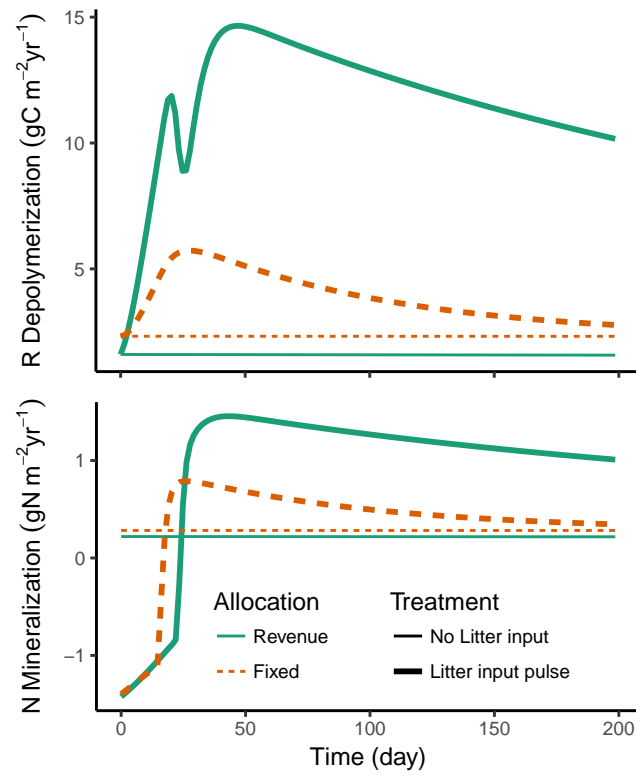


Figure 5: Priming experiment: Both depolymerisation of the residue substrate pool, R , and total N mineralization Φ were stimulated most strongly with the Revenue strategy after a subsoil has been amended with a pulse of fresh litter compared to a control with no amendment (thin horizontal lines).

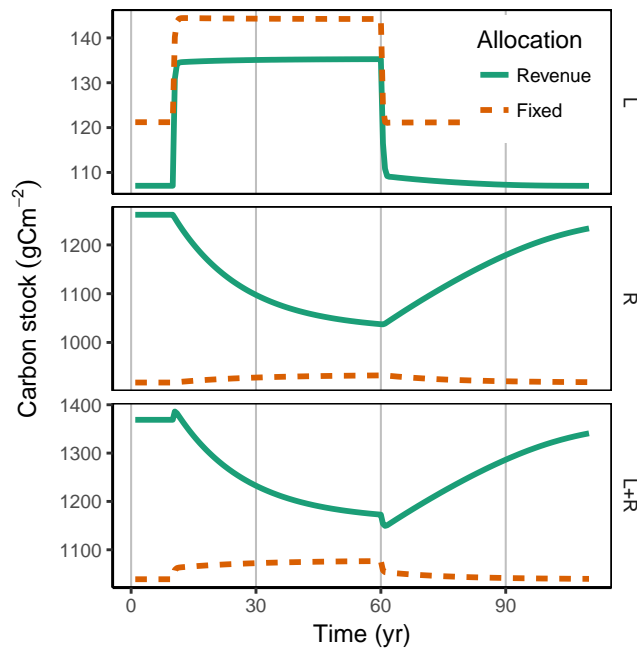


Figure 6: C-Stocks in the CO₂-Fertilization experiment: The Revenue strategy led to a mining, i.e. decrease, of the residue substrate pool, R during increased carbon litter inputs in years 10 to 60.

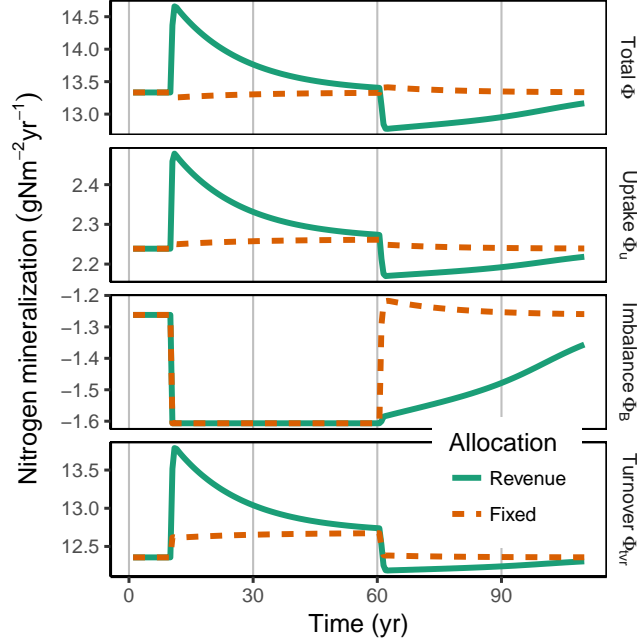


Figure 7: N Mineralization in the CO₂-Fertilization experiment: Mineralization of microbial turnover contributed most of the liberation of SOM-N with the Revenue strategy during microbial N limitation. After the end of the fertilisation at year 60, microbes with the Revenue strategy continued to more strongly immobilize N (negative flux Φ_B).

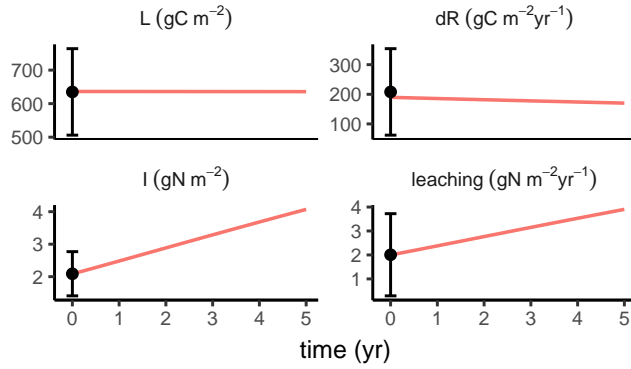


Figure 8: Calibrated SEAM predictions (lines) matched observations from the Laqueuille intensive pasture site (dots and standard deviation bars) of litter pool, L , change of SOM pools, dR , inorganic N, I , and N leaching rate.

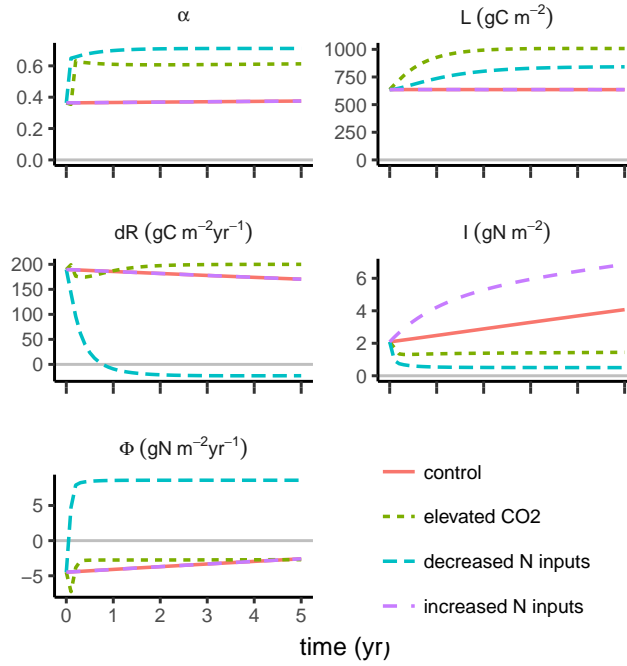


Figure 9: Simulated dynamics after prescribed alteration of C and N inputs for Laqueuille intensive pasture site: Shifts in enzyme allocation (α) led to changes in the evolution of organic and inorganic pools and N mineralization fluxes. Increased N substrate limitation, either due to elevated CO₂ or due to decreasing inorganic N inputs, caused a decrease in mineral N pool, I . If the substrate N limitation could not be balanced by inorganic N input, then the change rate of the residue pool, dR , decreased down to negative values, i.e. decreasing SOM pools.

678 Appendix A. SEAM equations

679 For an overview of symbol definitions see tables 1, A.5, and A.6.

680 Appendix A.1. Carbon fluxes

$$\frac{dB}{dt} = \text{syn}_B - \text{tvr}_B \quad (\text{A.1a})$$

$$\frac{dE_L}{dt} = (1 - \alpha) \text{syn}_E - \text{tvr}_{EL} \quad (\text{A.1b})$$

$$\frac{dE_R}{dt} = \alpha \text{syn}_E - \text{tvr}_{ER} \quad (\text{A.1c})$$

$$\frac{dL}{dt} = -\text{dec}_L + \text{input}_L \quad (\text{A.1d})$$

$$\frac{dR}{dt} = -\text{dec}_R + \epsilon_{\text{tvr}} \text{tvr}_B + (1 - \kappa_E)(\text{tvr}_{ER} + \text{tvr}_{EL}), \quad (\text{A.1e})$$

681 where α is the proportion of total investment into enzymes that is allocated
 682 to the residue pool R (section 2.3, input_L is the litter C input to the system,
 683 ϵ_{tvr}) is the fraction of microbial turnover C that is respired by predators, and
 684 κ_E is the fraction of enzyme turnover that is transferred to the DOM instead
 685 of the R pool. The specific fluxes are detailed below.

Total enzyme production syn_E , maintenance respiration r_M , and micro-
 bial turnover tvr_B are modelled as a first-order kinetics of biomass:

$$\text{syn}_E = a_E B \quad (\text{A.2a})$$

$$r_M = m B \quad (\text{A.2b})$$

$$\text{tvr}_B = \tau B \quad (\text{A.2c})$$

686 Enzyme turnover (tvr_{ER} and tvr_{EL}) is modelled as first-order kinetics of
 687 enzyme levels.

$$\text{tvr}_{ES} = k_E E_S, \quad (\text{A.3})$$

688 where S represents the litter L and residue R substrate pools, respectively.

Substrate depolymerisation is modelled first-order to substrate availability with a saturating Michaelis-Menten kinetics to enzyme levels:

$$\text{dec}_{S,Pot} = k_S S \quad (\text{A.4a})$$

$$\text{dec}_S = \text{dec}_{S,Pot} \frac{E_S}{K_{M,S} + E_S} \quad (\text{A.4b})$$

689 The DOM pool is assumed to be in quasi steady state, and hence, the
 690 sum of all influxes to the DOM pool (decomposition + part of the enzyme
 691 turnover) is taken up by microbial community.

$$u_C = \text{dec}_L + \text{dec}_R + \kappa_E (\text{tvr}_{ER} + \text{tvr}_{EL}) \quad (\text{A.5})$$

692 Under C limitation, C available for synthesis of new biomass and associ-
 693 ated catabolic growth respiration, C_{synBC} , is the difference between C uptake
 694 and expenses for enzyme synthesis (eq. A.2a) and maintenance respiration
 695 (eq. A.2b).

$$C_{\text{synBC}} = u_C - \text{syn}_E / \epsilon - r_M \quad (\text{A.6})$$

696 If the C balance for biomass synthesis, syn_B (eq. A.11), is positive, only a
 697 fraction ϵ , the anabolic carbon use efficiency, is used for synthesis of biomass
 698 and enzymes, whereas the rest is used for catabolic growth respiration r_G

699 to support this synthesis. For simplicity, the SEAM assumes ϵ to be the
700 same for all substrates. The model assumes that requirements for enzyme
701 synthesis and maintenance must be met. Hence, the microbial C balance can
702 become negative where microbial biomass starves and declines.

$$\text{syn}_B = \begin{cases} \epsilon C_{\text{synB}}, & \text{if } C_{\text{synB}} > 0 \\ C_{\text{synB}}, & \text{otherwise} \end{cases} \quad (\text{A.7a})$$

$$\text{r}_G = \begin{cases} (1 - \epsilon) C_{\text{synB}}, & \text{if } C_{\text{synB}} > 0 \\ 0, & \text{otherwise ,} \end{cases} \quad (\text{A.7b})$$

703 where C_{synB} is the C balance for biomass synthesis and is given below by eq.
704 A.11.

705 *Appendix A.2. Nitrogen fluxes*

706 Nitrogen fluxes and pools are derived by dividing the respective fluxes
707 with the C/N ratio, β , of their source.

The C/N ratios β_B and β_E of the microbial biomass and enzymes are assumed to be fixed. However, the C/N ratio of the substrate pools may

change over time and thus the substrate N pools are modelled explicitly.

$$\frac{dL_N}{dt} = -\text{dec}_L / \beta_L + \text{input}_L / \beta_i \quad (\text{A.8a})$$

$$\begin{aligned} \frac{dR_N}{dt} = & -\text{dec}_R / \beta_R + \epsilon_{\text{tvr}} \text{tvr}_B / \beta_B + \\ & (1 - \kappa_E)(\text{tvr}_{ER} + \text{tvr}_{EL}) / \beta_E \end{aligned} \quad (\text{A.8b})$$

$$\frac{dI}{dt} = +i_I - k_{IP} - lI + \Phi \quad (\text{A.8c})$$

$$\Phi = \Phi_u + \Phi_B + \Phi_{\text{tvr}} \quad (\text{A.8d})$$

$$\Phi_u = (1 - \nu)u_{N,OM}, \quad (\text{A.8e})$$

708 where the balance of the inorganic N pool I sums inorganic inputs i_I , plant
 709 uptake k_{IP} , leaching lI , and the exchange flux with soil microbial biomass, Φ .
 710 The latter is the sum of the apparent mineralization due to soil heterogeneity
 711 (Manzoni et al., 2008), Φ_u , mineralisation-immobilisation imbalance flux,
 712 Φ_B (A.12c), and mineralisation of a part of microbial turnover, Φ_{tvr} (A.14b,
 713 section Appendix A.5).

Organic N uptake, $u_{N,OM}$, was modelled as a parallel scheme (PAR), where a part of the organic N that is taken up from DON is mineralised at soil core scale accounting for imbalance flux at sub-scale soil spots with high N concentration in DOM (Manzoni et al., 2008). Potential N uptake is the sum of organic N uptake and the potential immobilisation flux ($u_{\text{imm,Pot}}$). Uptake from DOM is assumed equal to influxes to DOM times the apparent

N use efficiency ν .

$$u_N = \nu u_{N,OM} + u_{\text{imm,Pot}} \quad (\text{A.9a})$$

$$u_{N,OM} = \text{dec}_L / \beta_L + \text{dec}_R / \beta_R + \kappa_E (\text{tvr}_{ER} + \text{tvr}_{EL}) / \beta_E \quad (\text{A.9b})$$

$$u_{\text{imm,Pot}} = i_B I, \quad (\text{A.9c})$$

714 where C/N ratios β_L and β_R are calculated based on current C and N sub-
715 strate pools: $\beta_L = L/L_N$.

The N available for biomass synthesis is the difference of microbial N uptake and expenses for enzyme synthesis. This translates to a N constraint for the C used for biomass synthesis and its associated catabolic growth respiration: $C_{\text{synB}} \leq C_{\text{synBN}}$.

$$N_{\text{synBN}} = u_N - \text{syn}_E / \beta_E, \quad (\text{A.10a})$$

$$C_{\text{synBN}} = \beta_B N_{\text{synBN}} / \epsilon \quad (\text{A.10b})$$

716 *Appendix A.3. Imbalance fluxes of C versus N limited microbes*

717 There are constraints of each element on the synthesis of new biomass
718 and associated growth respiration. The minimum of these fluxes (eq. A.11)
719 constrains the synthesis of new biomass.

$$C_{\text{synB}} = \min(C_{\text{synBC}}, C_{\text{synBN}}) \quad (\text{A.11})$$

The excess elements are lost by imbalance fluxes (eq. A.12). The excess C is respired by overflow respiration, r_O , and the excess N is mineralised,

M_{Imb} , so that the mass balance is closed.

$$r_O = u_C - (\text{syn}_B + \text{syn}_E / \epsilon + r_G + r_M) \quad (\text{A.12a})$$

$$M_{\text{Imb}} = u_N - (\text{syn}_B / \beta_B + \text{syn}_E / \beta_E) \quad (\text{A.12b})$$

$$\Phi_B = M_{\text{Imb}} - u_{\text{imm,Pot}} \quad (\text{A.12c})$$

720 The actual mineralisation-immobilisation flux Φ_B is the difference be-
 721 tween the potential immobilisation flux and excess N mineralization. If
 722 microbes are limited by C availability, Φ_B will be positive, whereas with
 723 substrate N limitation, Φ_B will be a negative flux, corresponding to N immo-
 724 bilisation. With microbial N limitation, i.e. required immobilisation is larger
 725 than potential immobilisation, $\Phi_B = -u_{\text{imm,Pot}}$ and stoichiometry must be
 726 balanced by overflow respiration.

727 *Appendix A.4. Weight of an element limitation*

728 The weight of an element limitation is computed as the ratio between
 729 required uptake flux for given other constraints to the available fluxes for
 730 biosynthesis.

$$w_{\text{CLim}} = \left(\frac{\text{required}}{\text{available}} \right)^\delta = \left(\frac{C_{\text{synBN}}}{C_{\text{synBC}}} \right)^\delta \quad (\text{A.13a})$$

$$w_{\text{NLim}} = \left(\frac{\epsilon C_{\text{synBC}} / \beta_B}{N_{\text{synBN}}} \right)^\delta, \quad (\text{A.13b})$$

731 where parameter δ , arbitrarily set to 200, controls the steepness of the transi-
 732 tion between the two limitations. X_{synBY} denotes the available flux of element

733 X for biosynthesis and associated respiration given the limitation of element
 734 Y (A.6) and (A.10).

735 *Appendix A.5. Turnover mineralization fluxes*

In addition to mineralization flux due to stoichiometric imbalance, a part of microbial biomass is mineralised during microbial turnover, e.g. by grazing. A part $(1 - \epsilon_{\text{tvr}})$ of the biomass is used for catabolic respiration. With assuming that predator biomass elemental ratios do not differ very much from the one of microbial biomass, a respective proportion of N must be mineralized.

$$r_{\text{tvr}} = (1 - \epsilon_{\text{tvr}}) \text{tvr}_B \quad (\text{A.14a})$$

$$\Phi_{\text{tvr}} = (1 - \epsilon_{\text{tvr}}) \text{tvr}_B / \beta_B \quad (\text{A.14b})$$

736 All the non-respired turnover C enters the residue pool. In reality, a part
 737 of the microbial turnover probably enters the DOM pool again (e.g. by cell
 738 lysis) and is taken up again by microbial biomass. The increased uptake
 739 nearly cancels with an increased turnover. Hence, SEAM does not explicitly
 740 consider this shortcut loop so that fewer model parameters are required.
 741 Note, however, that turnover, uptake, and CUE in the model are slightly
 742 lower than in the real system where this shortcut operates.

Table A.5: Model parameters. The two value columns of initial values and parameter values refer to the prototypical examples and the Laqueuille pasture calibration respectively.

Symbol	Definition	Value		Unit	Rational
β_B	C/N ratio of microbial biomass	11	11	g g^{-1}	(Perveen et al., 2014)
β_E	C/N ratio of extracellular enzymes	3.1	3.1	g g^{-1}	(Sternner and Elser, 2002)
β_{input_L}	C/N ratio of plant litter inputs	30	70	g g^{-1}	(Perveen et al., 2014) ($1/\beta$)
k_R	maximum decomposition rate of R	1	4.39e-2	yr^{-1}	calibrated
k_L	maximum decomposition rate of L	5	1.95	yr^{-1}	calibrated
k_E	enzyme turnover rate	60	60	yr^{-1}	(Burns et al., 2013)
κ_E	fraction enzyme tvr. entering DOM instead R	0.8	0.8	(-)	mostly small proteins
a_E	enzyme production per microbial biomass	0.365	0.365	yr^{-1}	$\approx 6\%$ of biomass synthesis
K_M	enzyme half saturation constant	0.05	0.05	g m^{-2}	magnitude of DOC concentration
τ	microbial biomass turnover rate	6.17	6.17	yr^{-1}	(Perveen et al., 2014) (s/ϵ_{tvr})
m	specific rate of maintenance respiration	1.825	0	yr^{-1}	(van Bodegom, 2007), zero in (Perveen et al., 2014)
ϵ	anabolic microbial C substrate efficiency	0.5	0.53	(-)	calibrated
ν	aggregated microbial organic N use efficiency	0.7	0.9	(-)	(Manzoni et al., 2008)
ϵ_{tvr}	microbial turnover that is not mineralized	0.3	0.8	(-)	part of turnover is consumed by predators
i_B	maximum microbial uptake rate of inorganic N	25	25	yr^{-1}	larger than simulated immobilization flux
l	inorganic N leaching rate	-	0.959	yr^{-1}	(Perveen et al., 2014) (l)

Table A.6: Further symbols of quantities derived within the system

Symbol	Definition	Unit
α	proportion of enzyme investments allocated to production of E_R	(-)
syn_B	C for microbial biomass synthesis	$\text{g m}^{-2}\text{yr}^{-1}$
syn_{E_S}	C synthesis of enzymes degrading $S \in \{L, R\}$	$\text{g m}^{-2}\text{yr}^{-1}$
tvr_B	microbial biomass turnover C	$\text{g m}^{-2}\text{yr}^{-1}$
tvr_{E_S}	enzyme turnover C	$\text{g m}^{-2}\text{yr}^{-1}$
dec_S	C in depolymerization of resource $S \in \{L, R\}$	$\text{g m}^{-2}\text{yr}^{-1}$
u_C, u_N	microbial uptake of C and N	$\text{g m}^{-2}\text{yr}^{-1}$
$\Phi_u, \Phi_B, \Phi_{\text{tvr}}, \Phi$	N mineralization with microbial DOM uptake, stoichiometric imbalance, turnover, and total $\Phi = \Phi_u + \Phi_B + \Phi_{\text{tvr}}$ (Fig. 2)	$\text{g m}^{-2}\text{yr}^{-1}$

743 **Appendix B. Rationale behind the revenue strategy**

744 This section explains in a bit more detail, why allocating resources to
745 several enzymes proportional to the revenue is reasonable from a community
746 perspective

747 For a single microbe it would be optimal to maximise growth by investing
748 all resources in the enzyme that maximises the return per investment for
749 the currently limiting element. However, if many microbes compete for the
750 same best substrate, they also have to share the return of the extracellular
751 decomposition process. If another microbe targets the second-best substrate
752 at a different location by producing a different set of enzymes, it has an
753 advantage of first accessing the returns before those diffuse to the majority
754 of microbes located at the substrate with the highest revenue. When taking
755 this competition into account, it makes sense to allocate the most resources
756 for the best revenue but also some resources to the other possibilities. Hence,
757 the revenue strategy allocates resources proportional to their revenue. Note,
758 however, that this arguments assumes a DOM pool that is not completely
759 mixed, whereas SEAM employs the simplifying assumption of a single common
760 DOM pool.

761 Another argument draws from a similarity to the restriction of risk in
762 financial investments. It is reasonable to invest most into the best revenues,
763 but it is dangerous to invest solely in a single alternative. If the micro-
764 bial community expressed only one type of enzyme, resources might not be
765 sufficient to newly produce the other enzyme if the best resource becomes
766 unavailable, e.g. with changing pore connections with changing soil moisture.

767 Appendix C. Sensitivity to microbial turnover mineralization

768 The importance of N mineralization of microbial turnover, which is caused
769 mainly by predators that graze on microbes (Clarholm, 1985; Raynaud et al.,
770 2006), was one of the hypotheses in the development of the SEAM. This sec-
771 tion discusses SEAM’s sensitivity to parameterization of microbial turnover
772 mineralization.

773 To this end we performed the CO₂-Fertilization experiment using the
774 revenue strategy again with varying parameter ϵ_{tvr} , the part of microbial
775 turnover that is not mineralized. We also adjusted microbial anabolic effi-
776 ciency ϵ by the same but inverse factor so that simulation results start from
777 similar steady state of SOM stocks, which change with model parameteriza-
778 tion.

779 The change of the residue pool during the period of increased C inputs
780 was very similar across different parameterizations as long as the system
781 followed the same switches between several limitation states (Fig. C.10).
782 Contrary, if the re-parameterization shifted the system to different limita-
783 tion states then the dynamics changed qualitatively. For example with a
784 value of $\epsilon_{\text{tvr}} = 0.34$, there was an initial net N mineralization instead of N
785 immobilization, i.e. positive Φ_B (Fig. C.11). In the case of an initially large
786 difference between Φ_B and the maximum immobilization flux, the change
787 in amount and stoichiometry of litter inputs did not drive the system into
788 microbial N limitation ($-\Phi_B < u_{\text{immo},\text{Pot}}$). This case resulted in the absense
789 of the simulated decrease of the residue pool (Fig C.10). The high initial Φ_B
790 values resulted from the requirement that with the long term steady state,
791 the decomposer system must balance its organic litter N inputs by N miner-

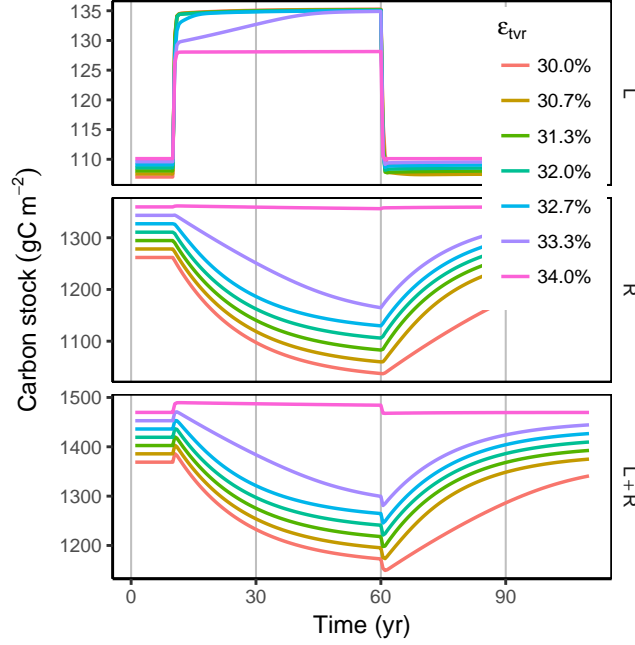


Figure C.10: C-Stocks in the CO₂-Fertilization experiment with varying mineralization of microbial turnover ($1 - \epsilon_{\text{tvr}}$): The patterns are similar, unless the system is shifted to another limitation regime.

792 alization. The required increase in litter C/N ratio that could shift a system
 793 simulated without turnover mineralization to N limitation was unreasonably
 794 large.

795 Hence, including the process of mineralization of microbial turnover is
 796 crucial to SEAM for simulating a reasonable dynamics for shifts between C
 797 and N limitation. Although the SEAM is not sensitive to the exact specifi-
 798 cation in turnover parameters if other parameters are recalibrated, there are
 799 thresholds than can drive the model to different stoichiometric limitations
 800 and can lead to substantial changes in model dynamics.

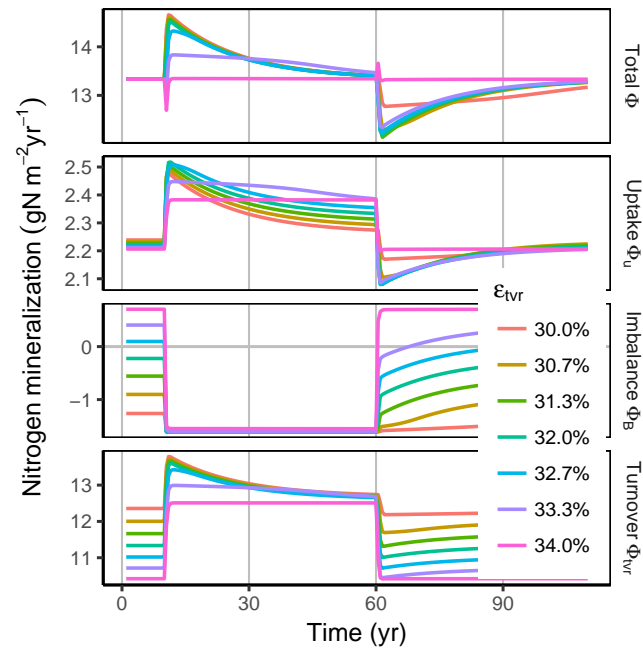


Figure C.11: N Mineralization in the CO₂-Fertilization experiment: Mineralization of microbial turnover contributed most of the liberation of SOM-N with the Revenue strategy during microbial N limitation. After the end of the fertilisation at year 60, microbes with the Revenue strategy continued to more strongly immobilize N (negative flux Φ_B).

801 *Acknowledgements* We thank Nazia Perveen and Sébastien Fontaine for
802 letting us reuse the data that they used for fitting the SYMPHONY model.
803 TW acknowledges support from Deutsche Forschungsgemeinschaft CRC 1076
804 “AquaDiva”. SZ acknowledges support from the European Research Council
805 (ERC) under the European Union’s Horizon 2020 research and innovation
806 programme (QUINCY; grant no. 647204).

807 **References**

- 808 Allard, V., Soussana, J.-F., Falcimagne, R., Berbigier, P., Bonnefond, J.,
809 Ceschia, E., D’hour, P., Hénault, C., Laville, P., Martin, C., Pinarès-
810 Patino, C., 2007. The role of grazing management for the net biome pro-
811 ductivity and greenhouse gas budget (co₂, {N₂O} and ch₄) of semi-natural
812 grassland. *Agriculture, Ecosystems & Environment* 121, 47 – 58.
- 813 Allison, S. D., Oct 2014. Modeling adaptation of carbon use efficiency in
814 microbial communities. *Frontiers in Microbiology* 5.
- 815 Allison, S. D., Vitousek, P. M., May 2005. Responses of extracellular enzymes
816 to simple and complex nutrient inputs. *Soil Biology & Biochemistry* 37 (5),
817 937–944.
- 818 Averill, C., Jul 2014. Divergence in plant and microbial allocation strategies
819 explains continental patterns in microbial allocation and biogeochemical
820 fluxes. *Ecology Letters* 17 (10), 1202–1210.
- 821 Averill, C., Rousk, J., Hawkes, C., Nov 2015. Microbial-mediated redistribu-
822 tion of ecosystem nitrogen cycling can delay progressive nitrogen limita-
823 tion. *Biogeochemistry* 126, 11–23.

- 824 Ballantyne, F., Billings, S., May 2014. Shifting resource availability, plastic
825 allocation to exoenzymes and the consequences for heterotrophic soil respi-
826 ration. In: EGU General Assembly Conference Abstracts. Vol. 16 of EGU
827 General Assembly Conference Abstracts. p. 16780.
828 URL <http://adsabs.harvard.edu/abs/2014EGUGA...1616780B>
- 829 Blagodatskaya, E., Khomyakov, N., Myachina, O., Bogomolova, I., Blago-
830 datsky, S., Kuzyakov, Y., Jul 2014. Microbial interactions affect sources of
831 priming induced by cellulose. *Soil Biology and Biochemistry* 74, 39–49.
- 832 Burns, R. G., DeForest, J. L., Marxsen, J., Sinsabaugh, R. L., Stromberger,
833 M. E., Wallenstein, M. D., Weintraub, M. N., Zoppini, A., 2013. Soil
834 enzymes in a changing environment: Current knowledge and future direc-
835 tions. *Soil Biology and Biochemistry* 58, 216 – 234.
- 836 Clarholm, M., Dec 1981. Protozoan grazing of bacteria in soil - impact and
837 importance. *Microbial Ecology* 7, 343–350.
- 838 Clarholm, M., 1985. Interactions of bacteria, protozoa and plants leading
839 to mineralization of soil nitrogen. *Soil Biology and Biochemistry* 17 (2),
840 181–187.
- 841 Cleveland, C. C., Liptzin, D., Aug 2007. C:n:p stoichiometry in soil: is there a
842 redfield ratio for the microbial biomass? *Biogeochemistry* 85 (3), 235–252.
- 843 Davidson, E. A., Samanta, S., Caramori, S. S., Savage, K., 2012. The dual
844 arrhenius and michaelis-menten kinetics model for decomposition of soil
845 organic matter at hourly to seasonal time scales. *Global Change Biology*
846 18 (1), 371–384.

- 847 Drake, J. E., Darby, B. A., Giasson, M.-A., Kramer, M. A., Phillips, R. P.,
848 Finzi, A. C., 2013. Stoichiometry constrains microbial response to root
849 exudation- insights from a model and a field experiment in a temperate
850 forest. *Biogeosciences* 10 (2), 821–838.
- 851 Drake, J. E., Gallet-Budynek, A., Hofmockel, K. S., Bernhardt, E. S.,
852 Billings, S. A., Jackson, R. B., Johnsen, K. S., Lichter, J., McCarthy, H. R.,
853 McCormack, M. L., Moore, D. J. P., Oren, R., Palmroth, S., Phillips, R. P.,
854 Pippen, J. S., Pritchard, S. G., Treseder, K. K., Schlesinger, W. H., DeLu-
855 cia, E. H., Finzi, A. C., 2011. Increases in the flux of carbon belowground
856 stimulate nitrogen uptake and sustain the long-term enhancement of forest
857 productivity under elevated CO₂. *Ecology Letters* 14 (4), 349357.
- 858 Fontaine, S., Henault, C., Aamor, A., Bdioui, N., Bloor, J., Maire, V., Mary,
859 B., Revailiot, S., Maron, P., Jan 2011. Fungi mediate long term seques-
860 tration of carbon and nitrogen in soil through their priming effect. *Soil*
861 *Biology and Biochemistry* 43 (1), 86–96.
- 862 Fontaine, S., Mariotti, A., Abbadie, L., Jun 2003. The priming effect of
863 organic matter: a question of microbial competition? *Soil Biology & Bio-*
864 *chemistry* 35 (6), 837–843.
- 865 Franklin, O., Näsholm, T., Högberg, P., Högberg, M. N., May 2014. Forests
866 trapped in nitrogen limitation - an ecological market perspective on ecto-
867 mycorrhizal symbiosis. *New Phytol* 203 (2), 657–666.
- 868 Friedlingstein, P., Meinshausen, M., Arora, V. K., Jones, C. D., Anav, A.,

- 869 Liddicoat, S. K., Knutti, R., 2014. Uncertainties in cmip5 climate projec-
870 tions due to carbon cycle feedbacks. *Journal of Climate* 27 (2), 511–526.
- 871 Janssens, I. A., Dieleman, W., Luyssaert, S., Subke, J.-A., Reichstein, M.,
872 Ceulemans, R., Ciais, P., Dolman, A. J., Grace, J., Matteucci, G., et al.,
873 Apr 2010. Reduction of forest soil respiration in response to nitrogen de-
874 position. *Nature Geosci* 3 (5), 315–322.
- 875 Kaiser, C., Franklin, O., Dieckmann, U., Richter, A., Mar 2014. Microbial
876 community dynamics alleviate stoichiometric constraints during litter de-
877 cay. *Ecol Lett* 17 (6), 680–690.
- 878 Kumar, A., Kuzyakov, Y., Pausch, J., Jun 2016. Maize rhizosphere priming:
879 field estimates using ^{13}C natural abundance. *Plant and Soil*.
- 880 Kuzyakov, Y., Friedel, J. K., Stahr, K., Oct 2000. Review of mechanisms and
881 quantification of priming effects. *Soil Biology & Biochemistry* 32 (11-12),
882 1485–1498.
- 883 Manzoni, S., Porporato, A., 2009. Soil carbon and nitrogen mineraliza-
884 tion: Theory and models across scales. *Soil Biology and Biochemistry* 41,
885 1355–1379.
- 886 Manzoni, S., Porporato, A., Schimel, J. P., May 2008. Soil heterogeneity in
887 lumped mineralization-immobilization models. *Soil Biology & Biochem-*
888 *istry* 40 (5), 1137–1148.
- 889 Moorhead, D. L., Lashermes, G., Sinsabaugh, R. L., 2012. A theoretical
890 model of c-and n-acquiring exoenzyme activities, which balances microbial

891 demands during decomposition. *Soil Biology and Biochemistry* 53, 133–
892 141.

893 Mooshammer, M., Wanek, W., Hämmerle, I., Fuchslueger, L., Hofhansl, F.,
894 Knoltsch, A., Schnecker, J., Takriti, M., Watzka, M., Wild, B., et al., Apr
895 2014a. Adjustment of microbial nitrogen use efficiency to carbon:nitrogen
896 imbalances regulates soil nitrogen cycling. *Nat Comms* 5.

897 Mooshammer, M., Wanek, W., Zechmeister-Boltenstern, S., Richter, A.,
898 2014b. Stoichiometric imbalances between terrestrial decomposer commu-
899 nities and their resources: mechanisms and implications of microbial adap-
900 tations to their resources. *Frontiers in Microbiology* 5.

901 Norby, R. J., Warren, J. M., Iversen, C. M., Medlyn, B. E., McMurtrie,
902 R. E., Sep. 2010. CO₂ enhancement of forest productivity constrained
903 by limited nitrogen availability. *Proceedings of the National Academy of*
904 *Sciences* 107 (45), 19368–19373.

905 Panikov, N. S., 2010. Microbial ecology. *Environmental Biotechnology*, 121–
906 191.

907 Perveen, N., Barot, S., Alvarez, G., Klumpp, K., Martin, R., Rapaport,
908 A., Herfurth, D., Louault, F., Fontaine, S., Apr 2014. Priming effect and
909 microbial diversity in ecosystem functioning and response to global change:
910 a modeling approach using the symphony model. *Glob Change Biol* 20 (4),
911 1174 – 1190.

912 Phillips, R. P., Finzi, A. C., Bernhardt, E. S., 2011. Enhanced root exudation

913 induces microbial feedbacks to n cycling in a pine forest under long-term
 914 CO₂ fumigation. *Ecology Letters* 14 (2), 187194.

915 R Core Team, 2016. R: A Language and Environment for Statistical Com-
 916 puting. R Foundation for Statistical Computing, Vienna, Austria.
 917 URL <https://www.R-project.org>

918 Rastetter, E. B., Feb 2011. Modeling coupled biogeochemical cycles. *Frontiers*
 919 in *Ecology and the Environment* 9 (1), 68 – 73.

920 Rastetter, E. B., Ågren, G. I., Shaver, G. R., May 1997. RESPONSES
 921 OF n-LIMITED ECOSYSTEMS TO INCREASED CO₂: a BALANCED-
 922 NUTRITION, COUPLED-ELEMENT-CYCLES MODEL. *Ecological Ap-*
 923 *plications* 7 (2), 444–460.

924 Raynaud, X., Lata, J. C., Leadley, P. W., Sep 2006. Soil microbial loop and
 925 nutrient uptake by plants: a test using a coupled c : N model of plant-
 926 microbial interactions. *Plant and Soil* 287 (1-2), 95–116.

927 Resat, H., Bailey, V., McCue, L. A., Konopka, A., Dec 2011. Modeling mi-
 928 crobial dynamics in heterogeneous environments: Growth on soil carbon
 929 sources. *Microbial Ecology* 63 (4), 883–897.

930 Rousk, J., Hill, P. W., Jones, D. L., Dec 2014. Priming of the decomposition
 931 of ageing soil organic matter: concentration dependence and microbial
 932 control. *Functional Ecology* 29 (2), 285–296.

933 Schimel, J. P., Weintraub, M. N., 2003. The implications of exoenzyme ac-
 934 tivity on microbial carbon and nitrogen limitation in soil: a theoretical
 935 model. *Soil Biology and Biochemistry* 35, 549–563.

936 Sinsabaugh, R. L., Hill, B. H., Follstad Shah, J. J., Dec 2009. Ecoenzymatic
937 stoichiometry of microbial organic nutrient acquisition in soil and sediment.
938 Nature 462 (7274), 795–798.

939 Sinsabaugh, R. L., Manzoni, S., Moorhead, D. L., Richter, A., Jul 2013. Car-
940 bon use efficiency of microbial communities: stoichiometry, methodology
941 and modelling. Ecology Letters 16 (7), 930–939.

942 Sterner, R. W., Elser, J. J., 2002. Ecological stoichiometry: the biology of
943 elements from molecules to the biosphere. Princeton University Press.

944 Thornton, P. E., Lamarque, J.-F., Rosenbloom, N. A., Mahowald, N. M., Dec
945 2007. Influence of carbon-nitrogen cycle coupling on land model response
946 to co₂ fertilization and climate variability. Global Biogeochemical Cycles
947 21 (4).

948 Todd-Brown, K. E. O., Hopkins, F. M., Kivlin, S. N., Talbot, J. M., Allison,
949 S. D., Jul. 2012. A framework for representing microbial decomposition in
950 coupled climate models. Biogeochemistry 109 (1-3), 19–33.

951 van Bodegom, P., May 2007. Microbial maintenance: A critical review on its
952 quantification. Microbial Ecology 53 (4), 513–523.

953 Wang, G., Post, W. M., Mayes, M. A., Jan 2013. Development of microbial-
954 enzyme-mediated decomposition model parameters through steady-state
955 and dynamic analyses. Ecological Applications 23 (1), 255–272.

956 Wieder, W. R., Bonan, G. B., Allison, S. D., Jul 2013. Global soil carbon
957 projections are improved by modelling microbial processes. Nature Climate
958 Change.

- 959 Wutzler, T., Reichstein, M., 2008. Colimitation of decomposition by sub-
960 strate and decomposers - a comparison of model formulations. *Biogeo-*
961 *sciences* 5 (3), 749–759.
- 962 Wutzler, T., Reichstein, M., Mar. 2013. Priming and substrate quality inter-
963 actions in soil organic matter models. *Biogeosciences* 10 (3), 2089–2103.
- 964 Xu, X., Schimel, J. P., Thornton, P. E., Song, X., Yuan, F., Goswami, S.,
965 2014. Substrate and environmental controls on microbial assimilation of
966 soil organic carbon: a framework for earth system models. *Ecology letters*
967 17 (5), 547–555.
- 968 Xu, X., Thornton, P. E., Post, W. M., Jun 2013. A global analysis of soil mi-
969 crobial biomass carbon, nitrogen and phosphorus in terrestrial ecosystems.
970 *Global Ecology and Biogeography* 22 (6), 737–749.
- 971 Zaehle, S., Dalmonech, D., Oct. 2011. Carbon-nitrogen interactions on land
972 at global scales: current understanding in modelling climate biosphere
973 feedbacks. *Current Opinion in Environmental Sustainability* 3 (5), 311–
974 320.
- 975 Zechmeister-Boltenstern, S., Keiblinger, K. M., Mooshammer, M., Penuelas,
976 J., Richter, A., Sardans, J., Wanek, W., May 2015. The application of
977 ecological stoichiometry to plant - microbial - soil organic matter transfor-
978 mations. *Ecological Monographs* 85 (2), 133–155.